Latency Aware IPv6 Packet Delivery Scheme over IEEE 802.15.4 based Battery-Free Wireless Sensor Networks

Yi-Hua Zhu[1], *Senior Member, IEEE*, Shu-Wei Qiu[1,2], Kai-Kai Chi[1], *Member, IEEE*, and Yuguang "Michael" Fang[3], *Fellow, IEEE*
[1]School of Computer Science and Technology, Zhejiang University of Technology, Hangzhou, Zhejiang 310023, China
[2]Department of Computer Science, Shantou Polytechnic, Shantou, Guangdong 515071, China
[3]Department of Electrical and Computer Engineering, University of Florida, USA

***Abstract*—Battery-Free Wireless Sensor Networks (BF-WSNs) have become increasingly useful for many applications and how to ensure timely information exchange between nodes in IP networks and those in BF-WSNs is indispensable. The 6LoWPAN protocol is usually used to deliver IPv6 packets over IEEE 802.15.4 based WSNs, and has resolved the size mismatching problem between IPv6 packets and 802.15.4 Medium Access Control (MAC) frames by using packet fragmentation scheme to break an IPv6 packet into multiple small pieces with each fitted into a single 802.15.4 MAC frame. Unfortunately, IPv6 packets in BF-WSNs may suffer from intolerable delay for timely reassembling back to IPv6 packets. In this paper, we present a Latency Aware IPv6 Packet Delivery (LAID) scheme to reduce such IPv6 packet latency while maintaining high packet delivery ratio. Our LAID considers charging time, data rate, and the Maximum Number of Transmission Trials (MNTT) used in the IEEE 802.15.4 MAC layer so that the minimum latency can be achieved by optimizing the pairing of data rate and MNTT. In addition, we apply network coding to improve packet delivery reliability. Our analysis shows that the proposed LAID significantly outperforms existing schemes with fixed data rates in terms of IPv6 packet latency.**

***Index Terms*—Latency, MAC, 6LoWPAN, battery-free wireless sensor networks, energy harvesting wireless sensor networks, Internet of Things (IoT).**

I. INTRODUCTION

NODES in traditional Wireless Sensor Networks (WSNs) are usually powered by batteries. In many applications, it is not convenient and even very difficult to replace batteries once a WSN is deployed. Therefore, Battery-Free WSNs (BF-WSNs) emerge. This paper focuses on BF-WSNs, in which sensor nodes do not have to have batteries but use various capacitors to harvest and store energy from ambience.

Normal energy sources in ambience include sunlight [1] [2], radio transmissions [3] [4], tremors, winds, piezoelectricity, and others [5]. Unlike traditional WSNs, BF-WSNs or Energy Harvesting WSNs (EH-WSNs) exhibit new characteristics [5] [6]. One of them is the intermittent and changeable energy source, which makes energy harvesting rate hard to accurately predict and residual energies of nodes fluctuate with time. Thus, data delivery in BF-WSNs proceeds intermittently because nodes have to switch to sleeping mode in order to harvest sufficient energies when their energies diminish below a threshold. Therefore, BF-WSNs face new challenges in data delivery [7].

Being major components of the Internet of Things (IoT), BF-WSNs are required to exchange information between various smart objects (such as sensors and actuators) with nodes in the Internet [8] [9]. Fortunately, the IPv6 over Low-Rate Wireless Personal Area Network (6LoWPAN) protocol [10] standardized by the Internet Engineering Task Force (IETF) can be used to address this issue. This protocol supports the nodes running IEEE 802.15.4 in BF-WSNs to deliver IPv6 packets. One of the main tasks in the 6LoWPAN protocol is to resolve the packet size mismatching problem, i.e., an entire IPv6 packet cannot be carried within a single 802.15.4 Medium Access Control (MAC) frame, because the Maximum Transmission Unit (MTU) of IPv6 packets generated in the global Internet is at least 1280 bytes whereas the size of 802.15.4 MAC frame is up to 127 bytes. With the fragmentation scheme introduced in the 6LoWPAN protocol, a gateway node, which is located at the boundary of an IP network and a BF-WSN, breaks an IPv6 packet into multiple small pieces fitted within a single 802.15.4 MAC frame. The IPv6 packet is reassembled at the destination when all pieces are received.

In IoT, numerous smart objects are deployed within a BF-WSN or an EH-WSN. The Internet users control them via commands encapsulated in an IPv6 packet. Unfortunately, the fragmentation scheme in the 6LoWPAN protocol may bring in intolerable packet delay and result in the serious problem that the commands may not be timely delivered to the destination. That is, the IPv6 packet cannot be reassembled because one or more of its pieces do not reach the destination on time, causing the command invalid after the IPv6 packet is reassembled at the destination or making smart objects malfunctioned. The main reasons causing this intolerable delay in an IPv6 packet are as follows: 1) at least one piece of the IPv6 packet is delayed because some nodes on the path connecting a source and a destination do not have sufficient energy for transmission and 2) at least one piece suffers from frequent retransmissions. Even worse, retransmission encounters shortage of power, which brings in greater delay. Furthermore, nodes also face the problem of making decision on choosing a proper data rate for transmission. The reason is that a higher data rate shortens the packet transmission time, but it may bring with a higher Bit Error Rate (BER), followed by frame retransmissions; whereas

This project is supported in part by National Natural Science Foundation of China under grant numbers 61432015, 61379124, and 61472367.

a lower data rate may lead to longer transmission time, which contributes packet delay, but it reduces the probability of retransmissions. In a word, it is important to design a packet delivery scheme that takes node's energy charging time, data rate, and retransmissions into account so that the end-to-end packet latency is minimized.

Although (re)transmission/acknowledgement (ACK) mechanism, i.e., ARQ mechanism, is applied in the IEEE 802.15.4 MAC layer, which uses the parameter called the maximum number of retransmissions in order to improve packet delivery reliability, it is still possible that one piece of the IPv6 packet fails to be delivered to the recipient over a lossy wireless link after the maximum number of retransmissions is performed. If this occurs, the entire IPv6 packet cannot be reassembled at the recipient, which will cause all the pieces, including those that have been correctly received, to be retransmitted. To overcome this problem, we apply network coding to encode all pieces of the IPv6 packet so that loss of some encoded packets does not prevent the recipient from reassembling the original IPv6 packet. Considering only around 81 bytes are left in the IEEE 802.15.4 MAC layer for carrying the upper layer data when the security header is present [11], we apply the network coding scheme as those in our previous study [12] [13], in which the coding vectors only consume a few bytes.

The main contributions of this paper can be summarized as follows:

1) We develop a Latency Aware IPv6-packet Delivery (LAID) Scheme for BF-WSNs to reliably deliver IPv6 packets with the minimum end-to-end latency. In addition to the retransmission/ACK scheme applied in the MAC layer, network coding is adopted in the LAID to further improve packet delivery reliability.

2) We derive the analytical results for the successful transmission probability of a MAC frame, the average transmission time of an IPv6 packet, the energy consumption of an IPv6 packet, and the IPv6 packet latency for the proposed LAID. Moreover, we also formulate the Optimization Problem (OP) that minimizes the IPv6 packet latency, which takes the energy charging time, the data rate and the Maximum Number of Transmission Trials (MNTT) of a MAC frame into account. The OP achieves the minimum latency (including capacitor charging time) while keeping a high Packet Delivery Ratio (PDR) by using proper pairing of data rate and MNTT. Extensive simulation results show that the proposed LAID significantly outperforms the existing schemes with fixed data rate and MNTT.

The remainder of this paper is organized as follows. Related works are surveyed in Section 2, and the LAID scheme is introduced in Section 3. The latency of an IPv6 packet in the LAID scheme and the OP minimizing the latency are presented in Section 4. The performance analyses are shown in Section 5. We conclude this paper in Section 6.

II. Related Works

Harvesting energy from ambience for BF-WSN or EH-WSN nodes has been intensively investigated. In [14] and [15], the energy harvesting process was assumed to be a Bernoulli process in which a device harvests energy with a fixed probability in each time slot. Ho *et al*. [16] considered the harvested energy as a stochastic process and proposed a generalized Markovian model in view of the random nature in solar and piezoelectric energy sources. Additionally, a Markov chain model was introduced in [17] to evaluate the proposed Robust Probabilistic Flooding (RPF). Ventura *et al*. [18] considered the case where the time interval of energy source occurrences is exponentially distributed. Khan *et al*. [19] proposed the Trinomial Random Walk (TRW) model for the storage capacity of energy harvesting enabled sensors, which was applied in a comprehensive solar radiation data set. Moreover, Kansal *et al*. [20] used a prediction model based on an Exponentially Weighted Moving-Average (EWMA) filter to exploit the diurnal cycle in solar energy. Piorno *et al*. [21] presented the solar prediction algorithm called Weather-Conditioned Moving Average (WCMA). Lin *et al*. [22] investigated the energy model that allows different energy sources in heterogeneous environments in which nodes can work with multiple energy sources. Seah *et al*. [7] derived the energy harvesting rate using difference technology on 10 cm^2 energy harvesting material. Tacca *et al*. [23] considered constant energy harvesting rates, i.e., a fixed amount of energy was harvested in each time slot. The results presented in the above surveyed works, however, may not be applicable to the contemporary WSNs that apply IEEE 802.15.4 standard in the MAC and physical layers because they do not take into account the data rates and the parameters used in the (re)transmission/ACK mechanism introduced in this standard.

To improve packet delivery in WSNs, various coding based schemes have been proposed. Mutschlechner *et al*. [24] used erasure codes to transmit information from mobile sensor nodes to stationary base station, and showed that the communication reliability could be considerably improved without impacting the resulting delay. Srouji *et al*. [25] proposed a reliable packet delivery scheme, called Reliable Data Transfer Scheme (RDTS), in which each intermediate node performs erasure coding and adaptively calculates the number of redundant packets for the next hop, and showed that RDTS does bring in longer network lifetime. Yang *et al*. [2] considered using solar energy surplus to adaptively adjust the redundancy level of erasure codes so that the packet delivery ratio can be improved without significantly impacting the network lifetime. Salhi *et al*. [26] developed the Reliable Coding for ZigBee (Re-CoZi) to enable robust XOR coding for WSNs to improve reliability using echo-feedback packet reception and decoding acknowledgement. In [27], a retransmission scheme based on an energy-efficient and network coding was presented, which enables the intermediate node to recover the lost packets such that the energy consumed for retransmissions is reduced. By considering the simultaneous use of gradient broadcast routing, fountain codes and intra-flow network coding, Apavatjrut *et al*. [28] proposed the XLT-GRAB strategy, which improves the reliability, the delay, and the network lifetime. Zhu *et al*. [29] used the enhanced Reed-Solomon (E-RS) code to achieve the minimum energy consumption while keeping data gathering ratio over a preset threshold.

To reduce latency, Luo and Sun [30] constructed the ar-

This is the author's version of an article that has been published in this journal. Changes were made to this version by the publisher prior to publication.
The final version of record is available at http://dx.doi.org/10.1109/TMC.2016.2601906

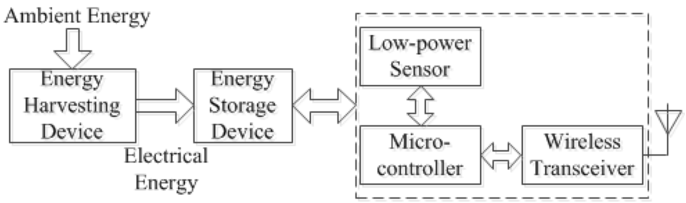

Fig. 1. The components of a BF-WSN node.

chitecture of an end-to-end communication system based on 6LoWPAN gateway, which features encapsulating 6LoWPAN adaptation layer in a network adapter driver in a personal computer, and showed that IPv6 hosts could be interactive with IP-based sensor nodes through 6LoWPAN gateway with acceptable latency and packet loss. Ludovici *et al*. [31] analyzed different routing solutions for 6LoWPANs such as ROR, MUR and enhanced ROR in terms of latency and energy consumption when transmitting IP fragmented packets. With a real commercial deployment, Hui *et al*. [32] showed that it is possible to simultaneously achieve an average duty cycle less than 0.4%, an average message delivery rate larger than 99.9%, and an average per-hop latency less than 125 ms over 12 months in different environments. Sagar *et al*. [33] introduced a passive wake-up radio device called range enhancing energy harvester mote, which uses the energy harvester circuit combined with an ultra-low-power pulse generator to trigger the wake-up of the mote so as to reduce the latency without increasing energy consumption.

The main difference between the proposed LAID and the above surveyed schemes is that in our LAID, capacitor charging time, data rate, and the parameters used in the retransmission/ACK mechanism in the 802.15.4 MAC layer are jointly optimized to achieve the minimum latency. Moreover, our LAID maintains high PDR and low energy consumption.

III. LAID Scheme

Before we describe the LAID in detail, we briefly describe the components of a BF-WSN node and the channel model first.

A. Components of a BF-WSN Node

Generally speaking, the node in our BF-WSN we consider here has an energy storage unit to store harvested energy, which enables the node to operate uninterruptedly in case when either the node fails to harvest energy from ambience or the amount of energy being harvested is not sufficient for its normal operation. The major components of a BF-WSN node are shown in Fig. 1 [34], where the components "Energy Harvesting Device" and "Energy Storage Device" are used to harvest and store energy, respectively. Usually, capacitor is used as the energy storage device. Hence, we use energy-harvesting time and capacitor charging time (or charging time for short) interchangeably.

B. Channel Model

We use (A_i, A_{i+1}) to represent the wireless link that connects nodes A_i and A_{i+1}, and $d_{i,i+1}$ for the distance between

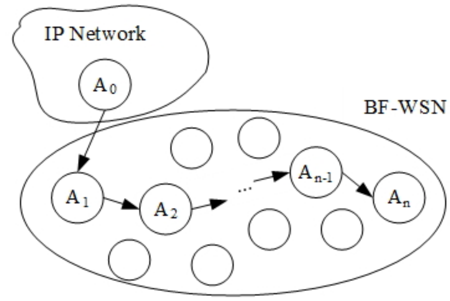

Fig. 2. An example of multi-hop packet delivery over a BF-WSN.

A_i and A_{i+1}. In the IEEE 802.15.4 system using Direct Sequence Spread Spectrum (DSSS) and Offset Quadrature Phase Shift Keying (O-QPSK) modulation, the BER of link (A_i, A_{i+1}) can be calculated by [35]

$$b_{i,i+1} = Q(\sqrt{2\psi(d_{i,i+1})B_N/R_i}), \tag{1}$$

where B_N is the noise bandwidth, R_i is the data rate for A_i,

$$Q(x) = \frac{1}{\sqrt{2\pi}} \int_x^{\infty} e^{-t^2/2} dt, x \geq 0 \tag{2}$$

and the received Signal to Noise Ratio (SNR) with distance $d_{i,i+1}$ is given by

$$\psi(d_{i,i+1}) = P_t - P_{lost}(d_0) - 10\eta \log_{10}(d_{i,i+1}/d_0) - P_{th}, \tag{3}$$

where P_t is the transmitted power, $P_{lost}(d_0)$ is the path loss at d_0 (=1m), η is the path loss exponent ranging from 2 to 4, and P_{th} is the noise power (or noise floor) in dB. The noise floor depends on the environment as well as time. To make the transmitted packet received successfully, the received power is required to be greater than P_{th}.

C. LAID Scheme

A gateway, which is located at the boundary of the IP network and our BF-WSN, is responsible for breaking IPv6 packet into small pieces with each suitable for a single MAC frame carried by BF-WSN nodes. In this paper, we classify the packets passing through the gateway into two categories: *down-going packets*, which traverse from the IP network to the BF-WSN, and *up-going packets*, which move in the opposite direction. Down-going packets usually contain commands to control BF-WSN nodes while up-going ones carry data sensed by BF-WSN nodes. Noticing that the up-going packets are small and can be carried within one IPv6 packet, i.e., it is not needed to break them up, we only consider delivering the down-going packets, which is illustrated in Fig. 2. In the figure, A_0 is the gateway and nodes A_1, A_2, $\ldots$, A_n stand for BF-WSN nodes. The route from the source A_0 to the destination A_n contains n hops through the intermediate nodes A_1, A_2, $\ldots$, and A_{n-1}.

In the 6LoWPAN protocol, Route-over Routing (ROR) and Mesh-under Routing (MUR) are introduced to deliver the fragments of an IPv6 packet. It has been shown in [12] that PDR, i.e., the probability of successfully delivering an IPv6 packet from source A_0 to destination A_n, under ROR is the same as that under MUR. Hence, without losing generality, we focus on ROR, in which the fragments are delivered in a hop-by-hop manner. That is, an IPv6 packet is fragmented and transmitted by A_0, and is reassembled at A_1 when all the fragments are successfully received. Then, the IPv6 packet is fragmented and transmitted again by A_1, and is reassembled at A_2. This process repeats until the IPv6 packet reaches A_n.

We refer to an IEEE 802.15.4 MAC frame as a BF-WSN frame below, which is no more than 127 bytes [36] whereas the payload of an IPv6 packet is usually greater than 1000 bytes. The LAID scheme, which is used to deliver the fragments of an IPv6 packet from the gateway to BF-WSN nodes, consists of two procedures: Proc_Gateway and Proc_mote. The former is used at the gateway while the latter is applied at BF-WSN nodes. In these procedures, node i $(i = 0, 1, \cdots, n-1)$ sets its MAC frame size (in bits) to

$$l_i = \max_{x\in\{1,2,\cdots\}} \{x | x < \frac{1}{b_{i,i+1}} - H_p, H_m + 10 \times 8 \leq x \leq 127 \times 8\}, \tag{4}$$

where $b_{i,i+1}$ is the BER of link (A_i, A_{i+1}) as given in (1), H_m represents the header size of BF-WSN MAC frame (in bits), and H_p is the PHY header size. From (4), we obtain $(l_i + H_p)b_{i,i+1} < 1, i = 0, 1, \cdots, n-1$. That is, the average number of erred bits resulting from transmitting an l_i-bit frame over each hop on the route from A_0 to A_n is less than 1, which aims to improve packet delivery reliability. In addition, $l_i \leq 127 \times 8$ guarantees that the size of a BF-WSN MAC frame is not greater than 127 bytes, which is required in the IEEE 802.15.4 standard; and $H_m + 10 \times 8 \leq l_i$ guarantees that the frame has at least 10 bytes of payload size. Then, node i breaks an IPv6 packet up into

$$s_i = \lceil L/(l_i - H_m) \rceil \tag{5}$$

fragments, where $\lceil \cdot \rceil$ is the ceiling function and L is the size of the IPv6 packet.

Moreover, for a given MAC frame, we use K_i to represent the MNTT applied at A_i to deliver the frame over link (A_i, A_{i+1}), which is the maximum number of transmissions permitted for the same frame, including the first transmission and the subsequent retransmissions. Then, the probability of successfully transmitting the l_i-bit MAC frame and the H_p-bit PHY header over link (A_i, A_{i+1}) with MNTT K_i is

$$p_{i,i+1} = 1 - [1 - (1 - b_{i,i+1})^{H_p + l_i}]^{K_i}, i = 0, 1, \cdots, n-1. \tag{6}$$

Noticing that the gateway is located at the IP network boundary, we assume the gateway does not apply energy harvesting. The main steps of Proc_Gateway, which is triggered when a down-going IPv6 packet reaches gateway A_0, are as follows:

Step 1. A_0 determines whether the IPv6 packet size L is greater than $l_0 - H_m$. If not, set $s_0 = 1$ and go to Step 3.

Step 2. A_0 breaks the IPv6 packet into s_0 fragments, where s_0 is given in (5).

Step 3. A_0 encodes the s_0 fragments to generate M_0 packets using the network coding scheme with the property that any s_0 of the M_0 encoded packets can recover the original fragments of the IPv6 packet [12] [24] [25], where

$$M_0 = min\Big\{ \Big\lceil \alpha \frac{s_0}{p_{0,1}} \Big\rceil, 30s_0 \Big\}. \tag{7}$$

Here, $p_{0,1}$ is the success probability of transmitting a frame with size of l_0 over link (A_0, A_1) and $\alpha \geq 1$ is a constant, called *redundant degree* of network coding. The role of α is to increase the number of encoded packets, which increases the probability that the recipient A_1 successfully receives s_0 encoded packets so that A_1 can retrieve the s_0 original fragments through decoding operation. We limit the number of encoded packets to 30 times of s_0 to avoid generating too more packets.

Step 4. Node A_0 determines its data rate R_0 and MNTT K_0 using the OP in (43).

Step 5. A_0 transmits the M_0 encoded packets to A_1 one after another with data rate R_0 and MNTT K_0 while counting the received ACK frames from A_1. A_0 stops transmitting and removes the encoded packets from the buffer upon it receives s_0 ACK frames.

Step 6. Stop.

Now, we explain the main steps in the above Proc_Gateway. In expression $s_0 = \lceil L/(l_0 - H_m) \rceil$, $l_0 - H_m$ is the payload size of the MAC frame used to carry data from the upper layers. In Step 3, $s_0/p_{0,1}$ in (7) is the expected number of transmissions performed at A_0 so that A_1 successfully receives s_0 encoded packets since $1/p_{0,1}$ is the average of transmissions performed by A_0 for one frame successfully received by A_1 with MNTT K_0. Constant α in (7) aims to increase the number of encoded packets, which improves the probability that A_1 decodes the s_0 original fragments of the IPv6 packet. Although a larger α leads to higher decoding probability, it consumes more buffer space in the sender. Hence, we limit $1 \leq \alpha \leq 2$.

The procedure Proc_mote used at node $A_i (i = 1, 2, \cdots, n-1)$ has the following steps:

Step 1. Node A_i acknowledges with an ACK frame to A_{i-1} as soon as it successfully receives a fragment from A_{i-1}. If the number of the received frames is equal to s_{i-1}, A_i decodes the original s_{i-1} fragments and reassembles the original IPv6 packet, from which the necessary information on routing the IP packet is obtained.

Step 2. Node A_i breaks the IPv6 packet into s_i fragments and encodes them into M_i packets using the network coding scheme with the property that any s_i of the encoded packets can recover the original fragments of the IPv6 packet [12] [24] [25]. Here, $M_i = min\{\lceil \alpha s_i / p_{i,i+1} \rceil, 30s_i\}$.

Step 3. Node A_i checks its energy storage device to see if the residual energy suffices to transmit. If not, A_i defers transmission until it harvests enough energy.

Step 4. Node A_i determines its data rate R_i and MNTT K_i using the OP in (43).

Step 5. Node A_i transmits the M_i encoded packets to A_{i+1} one after another with data rate R_i and MNTT K_i, counts the number of the ACK frames from A_{i+1}, and stops transmitting the remaining encoded packets when it has received s_i ACK frames from A_{i+1}.

Step 6. Stop.

TABLE I
PROBABILITY, TIME AND BIT IN TRANSMITTING A FRAGMENT AT A_i

TX trial	Status	Probability	Consumed Time	Transmitted bits
1st	Success	$q_{i,i+1}$	$\sigma_C + \frac{H_p+l_i}{R_i} + \sigma_A$	$H_p + l_i$
2nd	Success	$(1-q_{i,i+1})q_{i,i+1}$	$2(\sigma_C + \frac{H_p+l_i}{R_i}) + \sigma_T + \sigma_A$	$2(H_p + l_i)$
3rd	Success	$(1-q_{i,i+1})^2 q_{i,i+1}$	$3(\sigma_C + \frac{H_p+l_i}{R_i}) + 2\sigma_T + \sigma_A$	$3(H_p + l_i)$
$\cdots$	$\cdots$	$\cdots$	$\cdots$	$\cdots$
(K_i-1)th	Success	$(1-q_{i,i+1})^{K_i-2} q_{i,i+1}$	$(K_i-1)(\sigma_C + \frac{H_p+l_i}{R_i}) + (K_i-2)\sigma_T + \sigma_A$	$(K_i-1)(H_p + l_i)$
K_i-th	Success	$(1-q_{i,i+1})^{K_i-1} q_{i,i+1}$	$K_i(\sigma_C + \frac{H_p+l_i}{R_i}) + (K_i-1)\sigma_T + \sigma_A$	$K_i(H_p + l_i)$
	Failed	$(1-q_{i,i+1})^{K_i}$	$K_i(\sigma_C + \frac{H_p+l_i}{R_i} + \sigma_T)$	$K_i(H_p + l_i)$

To save the energy consumed by the intermediate nodes in solving the OP in (43), Step 4 in Proc_mote, which determines its data rate and MNTT, is conducted after fixed number of IPv6 packets are transmitted. That is, the pairing of data rate and MNTT from the OP's solution has been applied until the new pairing is determined.

In fact, there are various types of BF-WSNs in which nodes can harvest energy from ambient light such as sunlight, radio transmissions, and other energy sources. Generally speaking, the amount of energy harvested from sunlight is much more than that from radio transmissions, e.g., Wireless Identification Sensing Platform (WISP) [37]. Hence, in the applications with more harvested energy, we can let each intermediate node solve the OP to obtain its pairing of data rate and MNTT; while in the applications with less harvested energy, the pairing can be determined by gateways, which have the sufficient energy supply, and then a gateway delivers the pairing to the participating nodes. In fact, the pairing can be piggybacked on data packets.

It should be pointed out that the MNTT K_i and date rate R_i are the critical parameters in the procedures of Proc_Gateway and Proc_mote. It can be seen from (1) that R_i influences the BER $b_{i,i+1}$ over link (A_i, A_{i+1}) and further affects the success probability $p_{i,i+1}$. In general, as R_i increases, the time consumed in transmitting one bit decreases, but $p_{i,i+1}$ decreases; and the growth in K_i brings in high packet delivery ratio, but it may introduce longer delay. Therefore, how to set the optimal K_i and R_i to minimize packet latency is a critical problem in designing the LAID.

IV. IPv6 Packet Latency under the LAID Scheme

A. Timing in the LAID Scheme

In this section, we derive the latency for an IPv6 packet to be delivered from gateway A_0 to the destination A_n. As mentioned previously, an IPv6 packet is broken into s_0 fragments at A_0. We use ξ_i to represent the *preparation time* of an IPv6 packet at node $A_i (i = 1, 2, \cdots, n)$, which is defined as the duration from the instant when A_i receives the entire IPv6 packet from its preceding node A_{i-1} to the instant when A_i starts competing for the channel to transmit the first fragment of the IPv6 packet to its succeeding node A_{i+1}. In addition, we use T_i to represent the transmission time of the IPv6 packet at A_i, which is defined as the duration from the instant when A_i starts competing for the channel to transmit the first fragment to the instant when the entire IPv6 packet is transmitted to its succeeding node A_{i+1} (i.e., all fragments of the IPv6 packet are transmitted). Moreover, we denote by $t_i (i = 1, 2, \cdots, n)$ the i-hop duration of the packet, which is the time period from the instant when the IPv6 packet reaches gateway A_0 to the instant when the entire IPv6 packet is received by A_i. That is, t_i is the time for the packet to go over i hops. Especially, t_n is the latency of the IPv6 packet going from gateway A_0 to destination A_n. We refer to t_n as the end-to-end latency. The relations among t_i, ξ_i, and T_i are illustrated in Fig. 3.

From Fig. 3, we obtain

$$t_i = \sum_{j=0}^{i-1} (\xi_j + T_j), i = 1, 2, \cdots, n. \tag{8}$$

From (8), we obtain the expected end-to-end latency of an IPv6 packet as follows:

$$E[t_n] = \sum_{j=0}^{n-1} (E[\xi_j] + E[T_j]) \tag{9}$$

B. Transmission Time and Energy Consumption over One Hop

Next, we derive the transmission time T_i and the corresponding energy consumption over one hop. From Step 3 of Proc_Gateway and Step 5 of Proc_mote, which are presented in Section III, we are aware that: 1) node $i+1$ can recover the original IPv6 packet on the condition that the node receives s_i encoded packets; 2) node i stops transmitting the remaining encoded packets as soon as it receives s_i ACK frames; and 3) A_i generates totally M_i encoded packets and transmits them over link (A_i, A_{i+1}) one after another until A_{i+1} successfully receives s_i encoded packets $(i = 0, 1, \cdots, n-1)$.

1) Time and Energy Consumption of Transmitting a Fragment over One Hop

For a given fragment of the IPv6 packet at A_i, at most K_i transmission trials are performed. All possible transmission trials are summarized in Table I, where σ_C, σ_A and σ_T are the channel access time, the time consumed for the sender to

This is the author's version of an article that has been published in this journal. Changes were made to this version by the publisher prior to publication.
The final version of record is available at http://dx.doi.org/10.1109/TMC.2016.2601906

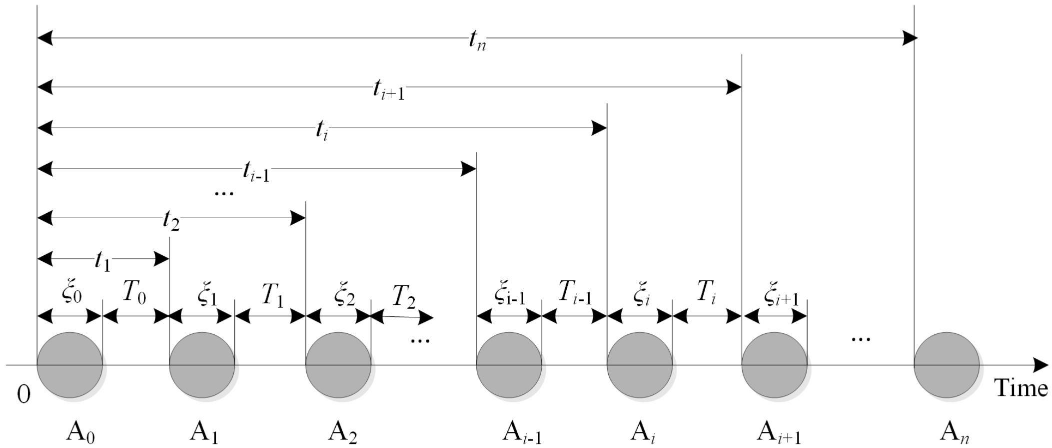

Fig. 3. Timeline of LAID.

receive the ACK frame from the recipient, and the value of the timer set at the sender for a transmitted frame (i.e., the frame is retransmitted if the sender does not receive its ACK frame), respectively. In addition, $q_{i,i+1}$ is the success probability of transmitting the fragment to A_{i+1} in one trial, i.e.,

$$q_{i,i+1} = (1 - b_{i,i+1})^{H_p + l_i}. \tag{10}$$

Now, we explain the main points in Table I. As one successful transmission trial suffices for the fragment, the j-th transmission trial takes place only when all the previous $j-1$ trials failed, which has the probability of $(1 - q_{i,i+1})^{j-1}$ and takes time $(j-1)(\sigma_C + \frac{H_p+l_i}{R_i} + \sigma_T)$ since each trial takes time σ_C in competing for the channel, time $(H_p + l_i)/R_i$ in transmitting the frame with l_i-bit PHY payload size plus H_p-bit PHY header size using data rate of R_i, and time σ_T for the expiration of the retransmission timer. Additionally, a successful transmission at the j-th trial has the probability $(1-q_{i,i+1})^{j-1} q_{i,i+1}$ and takes time $(j-1)(\sigma_C + \frac{H_p+l_i}{R_i} + \sigma_T) + (\sigma_C + \frac{H_p+l_i}{R_i} + \sigma_A) = j(\sigma_C + \frac{H_p+l_i}{R_i}) + (j-1)\sigma_T + \sigma_A (j = 1, 2, \cdots, K_i - 1)$, where σ_A is the time taken in receiving an ACK frame. Similarly, for the K_i-th trial, we can derive the last two rows in Table I.

From Table I, we obtain the expected time consumed for successfully transmitting the fragment from A_i to A_{i+1} with MNTT K_i as

$$\begin{aligned}
\eta_{i,i+1}^{(S)} &= \frac{1}{1 - (1 - q_{i,i+1})^{K_i}} \sum_{j=1}^{K_i} [(1 - q_{i,i+1})^{j-1} q_{i,i+1}] \\
&\quad [j(\sigma_C + \frac{H_p + l_i}{R_i}) + (j-1)\sigma_T + \sigma_A] \\
&= \frac{1}{1 - (1 - q_{i,i+1})^{K_i}} (\sigma_C + \frac{H_p + l_i}{R_i} + \sigma_T) \\
&\quad q_{i,i+1} \sum_{j=1}^{K_i} j(1 - q_{i,i+1})^{j-1} + (\sigma_A - \sigma_T) \\
&= \frac{1 - (1 - q_{i,i+1})^{K_i}(1 + K_i q_{i,i+1})}{q_{i,i+1}[1 - (1 - q_{i,i+1})^{K_i}]} \\
&\quad (\sigma_C + \frac{H_p + l_i}{R_i} + \sigma_T) + (\sigma_A - \sigma_T)
\end{aligned} \tag{11}$$

and the expected duration for the fragment failed over link of (A_i, A_{i+1}) with MNTT K_i as

$$\eta_{i,i+1}^{(F)} = K_i(\sigma_C + \frac{H_p + l_i}{R_i} + \sigma_T). \tag{12}$$

In addition, from Table I, we obtain the expected energy consumption for A_i to successfully transmit a fragment of the IPv6 packet to A_{i+1} with MNTT K_i as follows:

$$\begin{aligned}
\varepsilon_i^{TxD_S} &= \frac{1}{1 - (1 - q_{i,i+1})^{K_i}} \sum_{j=1}^{K_i} [(1 - q_{i,i+1})^{j-1} q_{i,i+1}] \\
&\quad [j(H_p + l_i)\theta_1] \\
&= \frac{1 - (1 - q_{i,i+1})^{K_i}(1 + K_i q_{i,i+1})}{q_{i,i+1}[1 - (1 - q_{i,i+1})^{K_i}]} (H_p + l_i)\theta_1,
\end{aligned} \tag{13}$$

where θ_1 is the energy consumption for transmitting one bit. In addition, the energy consumed by A_i when it fails in transmitting the fragment over link (A_i, A_{i+1}) with MNTT K_i is

$$\varepsilon_i^{TxD_F} = K_i \, (H_p + l_i) \, \theta_1. \tag{14}$$

Similarly, the expected energy consumption of A_i in successfully receiving a fragment of the IPv6 packet from A_{i-1} with MNTT K_{i-1} is

$$\begin{aligned}
\varepsilon_i^{RxD_S} &= \frac{1 - (1 - q_{i-1,i})^{K_{i-1}}(1 + K_{i-1} q_{i-1,i})}{q_{i-1,i}[1 - (1 - q_{i-1,i})^{K_{i-1}}]} \\
&\quad (H_p + l_{i-1})\theta_0
\end{aligned} \tag{15}$$

and the expected energy consumption of A_i failed in receiving a fragment of the IPv6 packet from A_{i-1} over link of (A_{i-1}, A_i) with MNTT K_{i-1} is

$$\varepsilon_i^{RxD_F} = K_{i-1}(H_p + l_{i-1})\theta_0, \tag{16}$$

where θ_0 is the energy consumption for receiving one bit. Here, θ_1 and θ_0 can be obtained using the energy consumption model presented in [38].

In addition, we obtain the expected energy consumption at A_i in transmitting the ACK frame to A_{i-1} to acknowledge the received fragment as

$$\varepsilon_i^{TxA} = (H_p + L_A)\theta_1, \tag{17}$$

where L_A is the size of ACK frame (in bits). Moreover, the expected energy consumption at A_i in receiving the ACK frame from A_{i+1} is

$$\varepsilon_i^{RxA} = (H_p + L_A)\theta_0. \tag{18}$$

2) Time and Energy Consumption for Transmitting IPv6 Packet over One Hop

The IP packet delivery has two outcomes: success and failure. The number of the encoded packets transmitted by A_i ranges from s_i to M_i. In the case when the outcome is success, exactly s_i of the M_i encoded packets are received since A_i stops transmission as soon as A_{i+1} receives s_i packets, whereas when it fails, at most $s_i - 1$ of them are received. Generally, in order to let A_{i+1} receive s_i packets, A_i may transmit $s_i + j$ encoded packets, where $j = 0, 1, \cdots, M_i - s_i$. The event that A_{i+1} receives s_i packets out of the $s_i + j$ encoded packets transmitted by A_i is equivalent to the event that A_{i+1} receives the last packet, i.e., the $(s_i + j)$-th packet, and exactly $s_i - 1$ out of the previous $s_i + j - 1$ packets. This event occurs with probability $\binom{s_i+j-1}{s_i-1}(p_{i,i+1})^{s_i-1}(1 - p_{i,i+1})^j p_{i,i+1} = \binom{s_i+j-1}{s_i-1}(p_{i,i+1})^{s_i}(1 - p_{i,i+1})^j$, and meanwhile A_i consumes time of $s_i\eta_{i,i+1}^{(S)} + j\eta_{i,i+1}^{(F)}$ and energy of $s_i(\varepsilon_i^{TxD_S} + \varepsilon_i^{RxA}) + j\varepsilon_i^{TxD_F}$, where $j = 0, 1, \cdots, M_i - s_i$. This is because a frame goes from A_i to A_{i+1} with successful probability $p_{i,i+1}$; and a successful packet transmission consumes time of $\eta_{i,i+1}^{(S)}$ and energy of $\varepsilon_i^{TxD_S} + \varepsilon_i^{RxA}$ whereas a failed packet transmission consumes time and energy as $\eta_{i,i+1}^{(F)}$ and $\varepsilon_i^{TxD_F}$, respectively. In the case when the outcome is failure, the event that j out of M_i packets are received occurs with probability $\binom{M_i}{j}(p_{i,i+1})^j(1 - p_{i,i+1})^{M_i-j}$, and it consumes time of $j\eta_{i,i+1}^{(S)} + (M_i - j)\eta_{i,i+1}^{(F)}$ and energy of $j(\varepsilon_i^{TxD_S} + \varepsilon_i^{RxA}) + (M_i - j)\varepsilon_i^{TxD_F}, j = 0, 1, \cdots, s_i - 1$.

As a result, under the condition that the IPv6 packet is successfully delivered to A_{i+1}, we have the expected transmission time $E[T_i]$ (see Fig. 3) as follows:

$$\begin{aligned} E[T_i] = &\frac{1}{\sum_{j=0}^{M_i-s_i}\binom{s_i+j-1}{s_i-1}(p_{i,i+1})^{s_i}(1-p_{i,i+1})^j} \\ &\sum_{j=0}^{M_i-s_i}\binom{s_i+j-1}{s_i-1}(p_{i,i+1})^{s_i}(1-p_{i,i+1})^j \\ &[s_i\eta_{i,i+1}^{(S)} + j\eta_{i,i+1}^{(F)}],\ i = 0, 1, \cdots, n-1. \end{aligned} \tag{19}$$

Additionally, the expected time consumed by A_i in transmitting the IPv6 packet to A_{i+1}, including both successful and failed transmissions, is as follows:

$$\begin{aligned} E[\tau_i] = &\sum_{j=0}^{M_i-s_i}\binom{s_i+j-1}{s_i-1}(p_{i,i+1})^{s_i}(1-p_{i,i+1})^j \\ &[s_i\eta_{i,i+1}^{(S)} + j\eta_{i,i+1}^{(F)}] + \sum_{j=0}^{s_i-1}\binom{M_i}{j}(p_{i,i+1})^j(1-p_{i,i+1})^{M_i-j} \\ &[j\eta_{i,i+1}^{(S)} + (M_i - j)\eta_{i,i+1}^{(F)}], i = 0, 1, \cdots, n-1. \end{aligned} \tag{20}$$

Similarly, under the condition that the IPv6 packet is successfully delivered to A_{i+1}, the expected energy consumption at A_i in transmitting the IPv6 packet to A_{i+1} and receiving the ACK from A_{i+1} is

$$\begin{aligned} E[\varepsilon_i^{Tx}] = &\frac{1}{\sum_{j=0}^{M_i-s_i}\binom{s_i+j-1}{s_i-1}(p_{i,i+1})^{s_i}(1-p_{i,i+1})^j} \\ &\sum_{j=0}^{M_i-s_i}\binom{s_i+j-1}{s_i-1}(p_{i,i+1})^{s_i}(1-p_{i,i+1})^j \\ &[s_i(\varepsilon_i^{TxD_S} + \varepsilon_i^{RxA}) + j\varepsilon_i^{TxD_F}], \\ &i = 0, 1, \cdots, n-1. \end{aligned} \tag{21}$$

The expected energy consumption at A_i in transmitting the IPv6 packet to A_{i+1} and receiving the ACK frames from A_{i+1}, including both successful and failed transmissions, is

$$\begin{aligned} E[e_i^{Tx}] = &\sum_{j=0}^{M_i-s_i}\binom{s_i+j-1}{s_i-1}(p_{i,i+1})^{s_i}(1-p_{i,i+1})^j \\ &[s_i(\varepsilon_i^{TxD_S} + \varepsilon_i^{RxA}) + j\varepsilon_i^{TxD_F}] \\ &+ \sum_{j=0}^{s_i-1}\binom{M_i}{j}(p_{i,i+1})^j(1-p_{i,i+1})^{M_i-j} \\ &[j(\varepsilon_i^{TxD_S} + \varepsilon_i^{RxA}) + (M_i - j)\varepsilon_i^{TxD_F}], \\ &i = 0, 1, \cdots, n-1. \end{aligned} \tag{22}$$

Likewise, under the condition that the IPv6 packet is successfully delivered from A_{i-1} to A_i, the expected energy consumption at A_i in receiving the IPv6 packet from A_{i-1} and acknowledging the received encoded packets to A_{i-1} is

$$\begin{aligned} E[\varepsilon_i^{Rx}] = &\frac{1}{\sum_{j=0}^{M_{i-1}-s_{i-1}}\binom{s_{i-1}+j-1}{s_{i-1}-1}(p_{i-1,i})^{s_{i-1}}(1-p_{i-1,i})^j} \\ &\sum_{j=0}^{M_{i-1}-s_{i-1}}\binom{s_{i-1}+j-1}{s_{i-1}-1}(p_{i-1,i})^{s_{i-1}}(1-p_{i-1,i})^j \\ &[s_{i-1}(\varepsilon_i^{RxD_S} + \varepsilon_i^{TxA}) + j\varepsilon_i^{RxD_F}], \\ &i = 1, 2, \cdots, n. \end{aligned} \tag{23}$$

Additionally, the expected energy consumption at A_i in receiving the IPv6 packet form A_{i-1} and acknowledging the received encoded packets to A_{i-1}, including both successful and failed transmissions, is

$$
\begin{aligned}
E[e_i^{Rx}] = &\sum_{j=0}^{M_{i-1}-s_{i-1}} \binom{s_{i-1}+j-1}{s_{i-1}-1}(p_{i-1,i})^{s_{i-1}} \\
&(1-p_{i-1,i})^j[s_{i-1}(\varepsilon_i^{RxD_S}+\varepsilon_i^{TxA})+j\varepsilon_i^{RxD_F}] \\
&+\sum_{j=0}^{s_{i-1}-1}\binom{M_{i-1}}{j}(p_{i-1,i})^j(1-p_{i-1,i})^{M_{i-1}-j} \\
&[j(\varepsilon_i^{RxD_S}+\varepsilon_i^{TxA})+(M_{i-1}-j)\varepsilon_i^{RxD_F}], \\
&i=1,2,\cdots,n. \qquad (24)
\end{aligned}
$$

In summary, the total energy expended by the source-to-destination route is

$$
\begin{aligned}
E[e^{Total}] &= E[e_0^{Tx}] + \sum_{i=1}^{n-1}(E[e_i^{Rx}]+E[e_i^{Tx}]) + E[e_n^{Rx}] \\
&= \sum_{i=0}^{n-1}E[e_i^{Tx}] + \sum_{i=1}^{n}E[e_i^{Rx}]. \qquad (25)
\end{aligned}
$$

Moreover, for $i = 0, 1, \cdots, n-1$, the probability that the IPv6 packet is successfully delivered over the $(i+1)$-hop, i.e., link (A_i, A_{i+1}), is $\sum_{j=0}^{M_i-s_i}\binom{s_i+j-1}{s_i-1}(p_{i,i+1})^{s_i}(1-p_{i,i+1})^j$, leading to the PDR over the n-hop source-to-destination route as follows:

$$
\delta_{PDR}^{(n)} = \prod_{i=0}^{n-1}\sum_{j=0}^{M_i-s_i}\binom{s_i+j-1}{s_i-1}(p_{i,i+1})^{s_i}(1-p_{i,i+1})^j. \qquad (26)
$$

C. The End-to-end Latency

Next, we begin to derive the expected end-to-end latency $E[t_n]$. We assume any node on the source-to-destination route forwards the IPv6 packet immediately after some necessary procedures (such as reassembling the packet) are performed. Compared to the time expended in data communication, computing time in a node can be ignored. In addition, for tractability, we do not consider the delay resulting from abnormal conditions, such as congestion occurrence, hardware failure, etc. Besides, we assume gateway A_0 does not harvest energy. Hence, ξ_0 in Fig. 3 can be ignored, i.e., $\xi_0 = 0$. Thus, $t_1 = T_0$. In node $\mathrm{A}_i (i = 1, 2, \cdots, n-1)$, packet preparation time ξ_i mainly includes the time consumed in recharging the energy storage device when the residual energy of the node is not sufficient for its transmissions.

For $i \in \{1, 2, \cdots, n\}$, we denote the residual energy of A_i at time t by $e_i(t)$; and the initial energy of A_i is set to e_0, which is sufficient to receive an IPv6 packet. In addition, we use $\underline{e}$ to denote the energy threshold and $\overline{e}$ the maximum energy the storage device holds. When the residual energy reaches $\overline{e}$, no more energy can be saved in the device. A node transmits the packet immediately once its residual energy is more than $\underline{e}$, which is assumed large enough for transmitting all M_i encoded packets. Moreover, we use function $g_i(t)$ to represent the instantaneous energy harvesting rate of A_i at time $t (i = 1, 2, \cdots, n)$.

Now, we study the residual energy of the nodes at times of $t_1, t_2, \cdots, t_n$ under the condition that the IPv6 packet is successfully delivered to the destination (i.e., all of its fragments are successfully delivered to the destination). From Fig. 3, we observe that at time t_1 the residual energy of A_1 is

$$
e_1(t_1) = min\{\overline{e}, e_0 + \int_0^{t_1} g_1(x)dx - E[e_1^{Rx}]\} \qquad (27)
$$

and the expected residual energy of the other nodes are

$$
e_j(t_1) = min\{\overline{e}, e_0 + \int_0^{t_1} g_j(x)dx\}, j = 2, 3, \cdots, n, \qquad (28)
$$

where $\int_0^{t_1} g_1(x)dx$ is the harvested energy during t_1, and $E[e_1^{Rx}]$, given in (24), is the expected energy consumption at node A_1 in receiving the s_0 fragments of the IPv6 packet and transmitting s_0 ACK frames. As a result, the preparation time ξ_1 is determined by

$$
\xi_1 = \begin{cases} 0, & \text{if } e_1(t_1) \geq \underline{e}; \\ min\{t | \int_{t_1}^{t_1+t} g_1(x)dx + e_1(t_1) > \underline{e}\}, & \text{otherwise.} \end{cases} \qquad (29)
$$

In the above expression, the first line indicates A_1 is able to transmit right away when its residual energy is over the threshold whereas the second line represents the charging time needed to harvest energy such that the residual energy is larger than the threshold $\underline{e}$.

At time t_2 when the IPv6 packet reaches A_2, the expected residual energies of A_1, A_2, and $\mathrm{A}_j (j = 3, 4, \cdots, n)$ can be expressed by (30)-(32).

$$
e_1(t_2) = min\{\overline{e}, e_0 + \int_0^{t_2} g_1(x)dx - E[e_1^{Rx}] - E[e_1^{Tx}]\}, \qquad (30)
$$

$$
\begin{aligned}
e_2(t_2) = min\{&\overline{e}, min\{\overline{e}, e_0 + \int_0^{t_1+\xi_1} g_2(x)dx\} \\
&+ \int_{t_1+\xi_1}^{t_2} g_2(x)dx - E[e_2^{Rx}]\}, \qquad (31)
\end{aligned}
$$

$$
e_j(t_2) = min\{\overline{e}, e_0 + \int_0^{t_2} g_j(x)dx\}, j = 3, 4, \cdots, n. \qquad (32)
$$

Additionally, the preparation time ξ_2 is determined by

$$
\xi_2 = \begin{cases} 0, & \text{if } e_2(t_2) \geq \underline{e}; \\ min\{t | \int_{t_2}^{t_2+t} g_2(x)dx + e_2(t_2) > \underline{e}\}, & \text{otherwise.} \end{cases} \qquad (33)
$$

At time t_3 when the IPv6 packet reaches A_3, node A_1 does not involve data delivery but charges its energy storage device. Hence, the residual energy of A_1 is

$$
e_1(t_3) = min\{\overline{e}, e_0 + \int_0^{t_3} g_1(x)dx - E[e_1^{Rx}] - E[e_1^{Tx}]\}; \qquad (34)
$$

the residual energy of A_2 changes to

$$
\begin{aligned}
e_2(t_3) = min\{&\overline{e}, min\{\overline{e}, e_0 + \int_0^{t_1+\xi_1} g_2(x)dx\} \\
&+ \int_{t_1+\xi_1}^{t_3} g_2(x)dx - E[e_2^{Rx}] - E[e_2^{Tx}]\}; \qquad (35)
\end{aligned}
$$

This is the author's version of an article that has been published in this journal. Changes were made to this version by the publisher prior to publication.
The final version of record is available at http://dx.doi.org/10.1109/TMC.2016.2601906

and the residual energy of A_3 is

$$e_3(t_3) = min\{\bar{e}, min\{\bar{e}, e_0 + \int_0^{t_2+\xi_2} g_3(x)dx\} + \int_{t_2+\xi_2}^{t_3} g_3(x)dx - E[e_3^{Rx}]\}. \quad (36)$$

Moreover, the residual energy of the other nodes are

$$e_j(t_3) = min\{\bar{e}, e_0 + \int_0^{t_3} g_j(x)dx\}, j = 4, 5, \cdots, n. \quad (37)$$

In addition, the preparation time ξ_3 is determined by

$$\xi_3 = \begin{cases} 0, & \text{if } e_3(t_3) \geq \underline{e}; \\ min\{t | \int_{t_3}^{t_3+t} g_3(x)dx + e_3(t_3) > \underline{e}\}, & \text{otherwise.} \end{cases} \quad (38)$$

Generally, we can derive the residual energy of the nodes at time t_i when the IPv6 packet is delivered to A_i. That is, at time t_i, the residual energy of A_1 is

$$e_1(t_i) = \begin{cases} min\{\bar{e}, e_0 + \int_0^{t_i} g_1(x)dx - E[e_1^{Rx}]\}, & i = 1; \\ min\{\bar{e}, e_0 + \int_0^{t_i} g_1(x)dx - E[e_1^{Rx}] - E[e_1^{Tx}]\}, \\ \qquad i = 2, 3, \cdots, n. \end{cases} \quad (39)$$

In addition, the residual energy of $\mathrm{A}_j (j = 2, 3, \cdots, n-1)$ is

$$e_j(t_i) = \begin{cases} min\{\bar{e}, e_0 + \int_0^{t_i} g_j(x)dx\}, & i \in [1, j-1]; \\ min\{\bar{e}, min\{\bar{e}, e_0 + \int_0^{t_{i-1}+\xi_{i-1}} g_j(x)dx\} \\ \quad + \int_{t_{i-1}+\xi_{i-1}}^{t_i} g_j(x)dx - E[e_j^{Rx}]\}, & i = j; \\ min\{\bar{e}, min\{\bar{e}, e_0 + \int_0^{t_{j-1}+\xi_{j-1}} g_j(x)dx\} \\ \quad + \int_{t_{j-1}+\xi_{j-1}}^{t_i} g_j(x)dx - E[e_j^{Rx}] - E[e_j^{Tx}]\}, \\ \qquad i \in [j+1, n]. \end{cases} \quad (40)$$

Moreover, the residual energy of A_n is

$$e_n(t_i) = \begin{cases} min\{\bar{e}, e_0 + \int_0^{t_i} g_n(x)dx\}, & i \in [1, n-1]; \\ min\{\bar{e}, min\{\bar{e}, e_0 + \int_0^{t_{n-1}+\xi_{n-1}} g_n(x)dx\} \\ + \int_{t_{n-1}+\xi_{n-1}}^{t_i} g_n(x)dx - E[e_n^{Rx}]\}, & i = n. \end{cases} \quad (41)$$

Furthermore, summarizing (29), (33), and (38), we obtain

$$\xi_i = \begin{cases} 0, & \text{if } e_i(t_i) \geq \underline{e}; \\ min\{t | \int_{t_i}^{t_i+t} g_i(x)dx + e_i(t_i) > \underline{e}\}, & \text{otherwise} \end{cases} \quad (42)$$

where $i = 1, 2, \cdots, n$.

As a result, the expected packet latency over n hops, i.e., the end-to-end latency $E[t_n]$ shown in (9), can be found when (19) and (42) are applied.

D. The Optimization Problem (OP)

To minimize the end-to-end packet latency $E[t_n]$, including the charging time, for an IPv6 packet delivery, we only need to minimize packet delay over each hop on the source-to-destination route. That is, node $\mathrm{A}_i (i = 0, 1, \cdots, n-1)$ uses the following OP to minimize end-to-end packet delay:

$$\begin{aligned} & min \quad E[T_i] + E[\xi_i] \\ & w.r.t. \quad K_i, R_i \\ & s.t. \begin{cases} K_i \in \{1, 2, \cdots, 8\}; \\ R_i \in \Omega. \end{cases} \end{aligned} \quad (43)$$

In the OP, the MNTT K_i takes a value in the set of $\{1, 2, \cdots, 8\}$ as the maximum number of retransmissions is set to 7 in the IEEE 802.15.4 standard; Ω is the set of available data rates supported by the IEEE 802.15.4g standard; and $E[T_i]$ and $E[\xi_i]$ are given in (19) and (42), respectively. The OP can be simply solved by enumeration because the number of feasible pairs of K_i and R_i are quite small.

V. Performance Evaluation

According to the IEEE 802.15.4 standard [36], a node contends for a channel before transmission, which consumes time of σ_C. In the standard, a backoff algorithm requires the node to randomly pick a Backoff Counter (BC) in the set $\{0, 1, \cdots, 2^{BE} - 1\}$, where *BE* is the exponential backoff initialized to the value of the parameter *MacMinBE* defined in the MAC layer [36], and then the node defers for BC slots each having a length of *aUnitBackoffPeriod* symbol periods. Thus, when the channel is idle, the average backoff time of the node is $(2^{BE} - 1)/2$ slots. The experiments in [39] showed that in a small-scale network, a node needs 1 backoff on average; and even in a network with 3000 nodes, a node needs approximately 1.5 backoffs on average. Hence, we assume the average number of backoffs is 1 in our study, which yields

$$\sigma_C = \frac{2^{BE} - 1}{2} UBP + CCA. \quad (44)$$

Here, *UBP* stands for *aUnitBackoffPeriod*; and *CCA* means Clear Channel Assessment, which is the time required to assess an idle channel in the PHY layer.

Considering O-QPSK-A modulation introduced in the IEEE 802.15.4g standard [40] supports multi-rate transmissions, we adopt the PHY layer that applies O-QPSK-A modulation over the 868-870 MHz frequency band, which has 4 data rates of 6.25, 12.5, 25, 50 kbps so that $\Omega = \{6.25, 12.5, 25, 50\}$ in (43). With this modulation, the symbol period is 320 μs, and *CCA* takes 4 symbol periods. Moreover, the default values of *MacMinBE* and *aUnitBackoffPeriod* are 3 and 20, respectively [40]. Thus, from (44), we have $\sigma_C = [(2^3 - 1)/2 \times 20 + 4] \times 320 = 23680\ \mu s$.

With O-QPSK-A PHY, the value of the timer for a transmitted frame, i.e., σ_T, is set to parameter *macAckWaitDuration*, which is equal to the sum of the parameters *aUnitBackoffPeriod*, *aTurnaroundTime*, *phySHRDuration*, *phyPHRDuration*, and *phyPSDUDuration*. Here, *aTurnaroundTime* is the RX-to-TX (receiver-to-transmitter) or TX-to-RX turnaround time, *phySHRDuration* is the duration of the synchronization header (SHR) in the PHY, *phyPHRDuration* is the duration of the PHY header (PHR), and *phyPSDUDuration* is the duration of an ACK frame [40]. Moreover, *phySHRDuration* and *phyPHRDuration* take 48 and 15 symbol periods, respectively; and *aTurnaroundTime* = 1000 μs. Furthermore, *phyPSDUDuration*

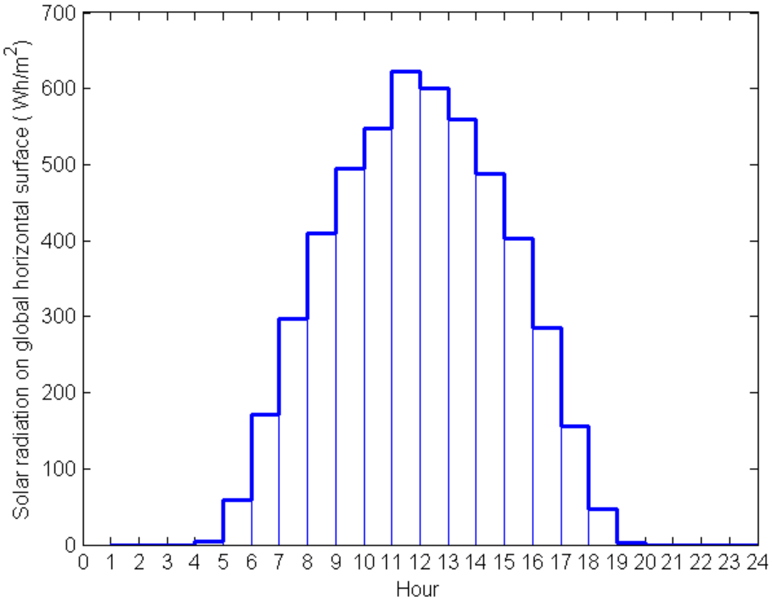

Fig. 4. The average solar radiation received on horizontal surface per hour.

TABLE II
PARAMETERS

Parameter	Value	Parameter	Value
P_t	1 dBm	H_p	9 B
B_N	30 kHz	H_m	39 B
$P_{lost}(d_0)$	55 dB	L_A	5 B
η	2	$\overline{e}$	1 J
P_{th}	-98 dBm	$\underline{e}$	0.5 J
α	2	e_0	0.3 J

$= (L_A/6250) \times 10^6 = 6400\ \mu$s, where L_A is the size of ACK frame in bits, i.e., L_A = 40 bits, and the lowest data rate, i.e., 6.25 kbps, is applied to reduce the loss probability of the ACK frame. As a result, $\sigma_T = 20 \times 320 + 1000 + 48 \times 320 + 15 \times 320 + 6400 = 33960\ \mu$s. In addition, we adopt the following default values: *macMaxFrameRetries* = 3, which leads to MNTT = 4; and *aMaxPHYPacketSize* = 127, which is the maximum size of PHY Service Data Unit (PSDU) in the PHY layer [36]. Considering the MTU is 1280 bytes in the IPv6 protocol, we choose IPv6 packet size as $L = 1300$ bytes [41]. The rest of the parameters are summarized in Table II.

As for energy harvesting rate, similar to [42], we use the solar irradiation data for Chicago O'Hare International Airport from the National Solar Radiation Data Base, which was published by The U.S. Department of Energy [43]. The average over data of direct and diffuse solar radiation received on a global horizontal surface during the 60-minute period in June, July and August of 2010 yield Fig. 4. From the figure, we observe that there is no solar radiation during periods of 0:00-4:00 and 20:00-24:00. It should be stressed that, the data shown in Fig. 4 are on 60-minute period basis, e.g., the peak of the figure indicates that the 60-minute period lasting from 11:00 to 12:00 can harvest energy of 623 Wh. Equivalently, 623 Ws (i.e., Joule) can be harvested for each second during period of 11:00 to 12:00. Considering that a sensor node has small size, we assume the surface of the device used to capture solar energy is a square with side of 2 cm, i.e., its area is 4 cm^2 or one 2500th of 1 m^2. Thus, in the simulation, we divide the data in Fig.4 by 2500. Especially, we study three cases with the lowest, medium, and the highest amount of harvested energy, which take the data during 19:00-20:00, 7:00-8:00, and 11:00-12:00, respectively. Thus, we have the energy harvesting rate function shown in (45), where the units of x and $g(x)$ are second and Joule, respectively, and the notation of (7:00, 8:00] represents the period of 7:00 (exclusive) to 8:00 (inclusive). In (45), the function values are represented in fraction whose numerator is the same as the corresponding value in Fig. 4 and the 2500 in the denominator is for the square device surface with side of 2 cm.

$$g(x) = \begin{cases} 296.40/2500, & x \in (7:00, 8:00]; \\ 623.30/2500, & x \in (11:00, 12:00]; \\ 1.93/2500, & x \in (19:00, 20:00]. \end{cases} \tag{45}$$

Moreover, we apply the energy consumption model presented in [38], from which $\theta_1 = E_{elec} + \varepsilon_{fs} d^2$ and $\theta_0 = E_{elec}$, where d is the distance between the transmitter and the receiver, $E_{elec} = 50$ nJ/bit, and $\varepsilon_{fs} = 10$ pJ/bit/m^2.

Considering the expected transmission time $E[T_i]$ in (19), the total energy consumption in (25) and PDR in (26) play important roles in the LAID, we first verify them via simulation. In the simulation, we set radio range to 10, 20, 30, and 40 m, respectively. In addition, we randomly generate source-to-destination paths with 10, 20, $\cdots$, and 50 hops, respectively. The distance of the two neighboring nodes is randomly generated to meet the given radio range (the distance is regenerated if it is greater than the given radio range). In each path, we let the source node deliver 3000 IPv6 packets to

This is the author's version of an article that has been published in this journal. Changes were made to this version by the publisher prior to publication.
The final version of record is available at http://dx.doi.org/10.1109/TMC.2016.2601906

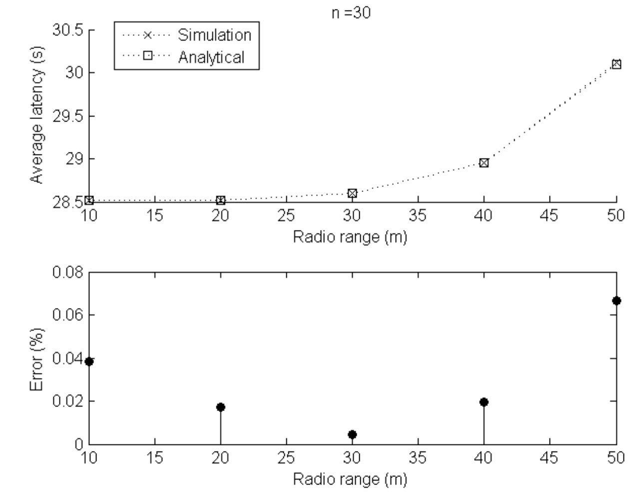

(a) Latency excluding the charging time vs radio range.

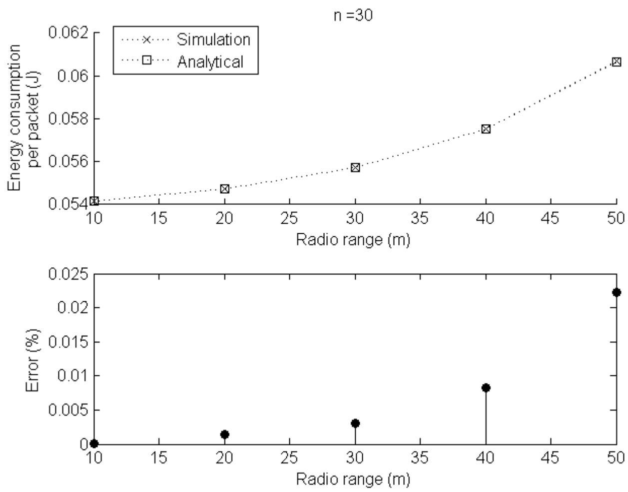

(b) Energy consumption vs radio range.

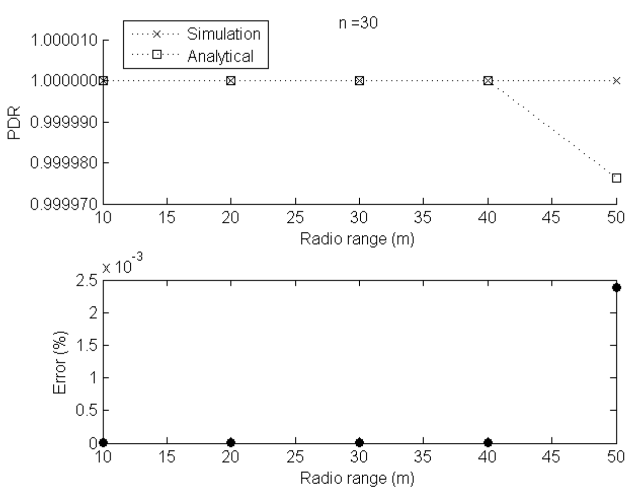

(c) PDR vs radio range.

Fig. 5. Comparison of simulation and analytical results.

the destination. All the results shown in the subsequent figures are from the average values over the 3000 packet deliveries. Additionally, the simulation results indicate that, for the three energy harvesting rates in (45), the latency of the LAID shares similar tendency. So do the energy consumption and PDR of the LAID. Hence, we only present the results when the first line of (45) is applied, which is a moderate value. That is, the energy harvesting rate $g(x) = 296.40/2500 = 0.11856$ J/s.

The simulation and analytical results of the end-to-end IPv6 packet latency, the energy consumption, and the PDR under the LAID are shown in Fig. 5(a), Fig. 5(b), and Fig. 5(c), respectively. The upper parts of the figures compare the simulation results with the analytical ones derived directly from (19), (25), and (26), while the lower parts show the errors of them. Here, we define the error as $|(x-y)/x|$, where x and y are the analytical and the simulation values, respectively. From Fig. 5, it can be clearly seen that the simulation and analytical results for latency, energy consumption, and PDR match very well because the errors are small. We are happy to see that PDR of the LAID is close to 1 (see Fig. 5(c)), which indicates the LAID is with very high reliability in packet delivery. We owe the high reliability to the network coding that encodes all the fragments of an IPv6 packet into multiple packets so that the receiving nodes are able to receive sufficient number of encoded packets to recover the ongoing IPv6 packet regardless of losing some encoded packets. It should be pointed out that, the packet latency shown in Fig. 5(a) does not include the charging time due to (19) excluding charging time.

Next, we compare the LAID with four schemes, each of which picks a Fixed Data Rate (FDR) in $\Omega = \{6.25, 12.5, 25, 50\}$ for transmissions. Accordingly, they are referred to as FDR6.25, FDR12.5, FDR25, and FDR50, respectively. In the FDR schemes, we set MNTT =4, i.e., the maximum number of retrials in the MAC layer defaults to 3.

Setting the radio range to 10, 20, 30, 40, 50, respectively, we obtain Fig. 6, in which EHR stands for energy harvesting rate. This figure compares the LAID with FDR6.25, FDR12.5, FDR25, and FDR50 in terms of packet latency (including capacitor charging time) and the energy consumption. From Fig. 6(a), we observe that: 1) the LAID achieves the best latency, which fulfills the aim of this paper; and 2) increase in radio range almost does not affect latency (it only brings with slight increase in latency), which agrees with our intuition because radio propagates in ray velocity so that time expended in traversing tens of meters can be ignored. Fig. 6(b) illustrates that: 1) the energy consumptions of all the schemes share the same increasing trend, i.e., the greater radio range the more energy consumption; and 2) their energy consumptions are very close (see Fig. 6(c)). In a word, the LAID is able to achieve much smaller packet delay than the FDR schemes by using nearly the same energy as them.

Setting the number of hops, i.e., n, to 10, 20, 30, 40, 50, respectively, we obtain Fig. 7, where R stands for the radio range. From Fig. 7 we observe that, with variation of n, the LAID remains the best in latency (see Fig. 7(a)) while its energy consumption is close to the other four schemes (see Fig. 7(b)). Moreover, increase in n causes the latency and the energy consumption of all the schemes to increase. This is because the IPv6 packet has to traverse more hops before it reaches the destination, resulting in higher packet latency and expending more energy.

Finally, we want to stress that, as mentioned previously, the PDRs of all the schemes are close to 1 (see Fig. 5(c)). So, we omit the figures for PDR.

VI. Conclusion

With the advances in IoT, Battery-Free Wireless Sensor Networks (BF-WSNs) have been widely deployed for many applications. One of the important communication tasks is to exchange information between nodes in the Internet and the BF-WSN nodes in order to integrate BF-WSNs into the Internet, one of the visions for IoT. Due to the huge number of envisioned communications devices connected to future Internet, IPv6 have to be used in the future. Unfortunately, IPv6 packets tend to have large size, and an IPv6 packet may not be fitted in an MAC frame for most wireless sensor networks, including BF-WSNs, without fragmentation. In fact, the 6LoWPAN protocol, which is standardized by the Internet Engineering Task Force (IETF) to deliver IPv6 packets over IEEE 802.15.4 standard based WSNs, adopts fragmentation technique. Unfortunately, with the 6LoWPAN protocol, end-to-end packet latency may be intolerable, which may cause IPv6 packets unable to reach the destination on time.

The possible factors affecting end-to-end packet latency in BF-WSNs are as follows. Firstly, packet delivery has to proceed in intermittent way. This is because the nodes have to enter low power mode to save and harvest energy when their residual energy are below threshold, which temporarily terminates the packet delivery, and wake up when they have sufficient energy for transmitting, which resumes the packet delivery. Secondly, packet delivery suffers from loss due to unreliable wireless links because the nodes are usually not able to transmit with high power level so that wireless links between the nodes prone to being broken, which may cause a fragment of the ongoing IPv6 packet unable to be delivered to a neighboring node even when the fragment is retransmitted with the greatest allowed parameter of *maximum number of transmission retrials* set in the MAC layer, thus preventing the destination from reassembling the original IPv6 packet. Therefore, how to efficiently deliver large-sized IPv6 packets over BF-WSNs suitable for small-sized packets is important and challenging, and should be carefully investigated. In this paper, we have addressed this important problem and have designed a Latency Aware IPv6 Packet Delivery (LAID) scheme to be implemented at the gateway nodes, which are located at the boundaries of the Internet and the BF-WSNs, and the nodes in the BF-WSNs in order to deliver IPv6 packets over the BF-WSNs in lowest latency. Through extensive evaluation, we have demonstrated that our LAID can considerably reduce the end-to-end packet latency over BF-WSNs by tuning the data rate and the MNTT in the MAC layer in BF-WSNs while maintaining high packet delivery ratio and consuming low harvested energy. We owe the high reliability, measured by PDR, to the network coding applied in the LAID, which encodes all fragments of an IPv6 packet into multiple packets

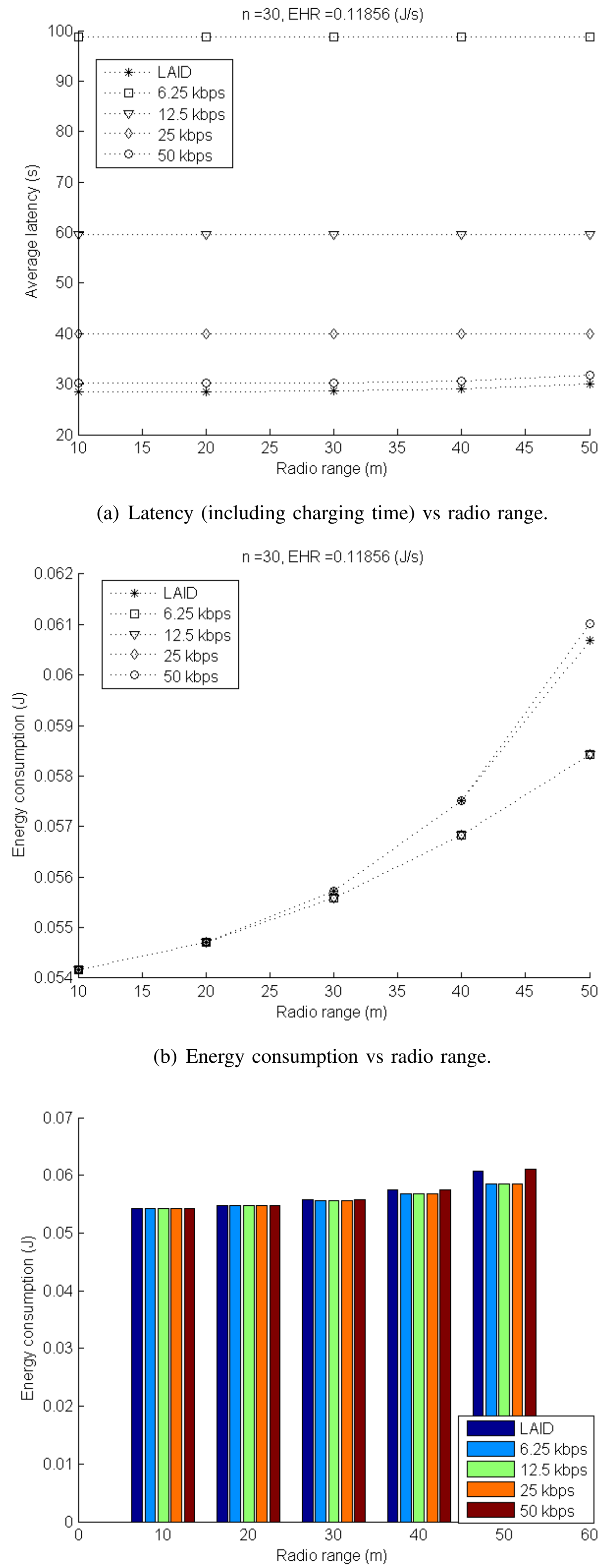

(a) Latency (including charging time) vs radio range.

(b) Energy consumption vs radio range.

(c) Energy consumption vs radio range (bar graph).

Fig. 6. Comparison of LAID, FDR6.25, FDR12.5, FDR25, and FDR50 when radio range varies.

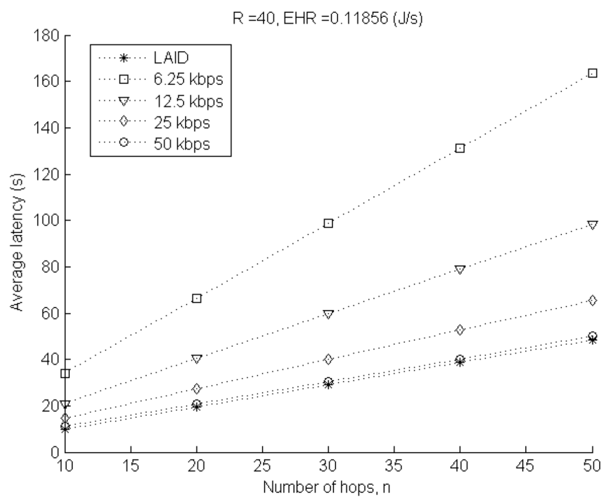

(a) Latency including the charging time vs the number of hops.

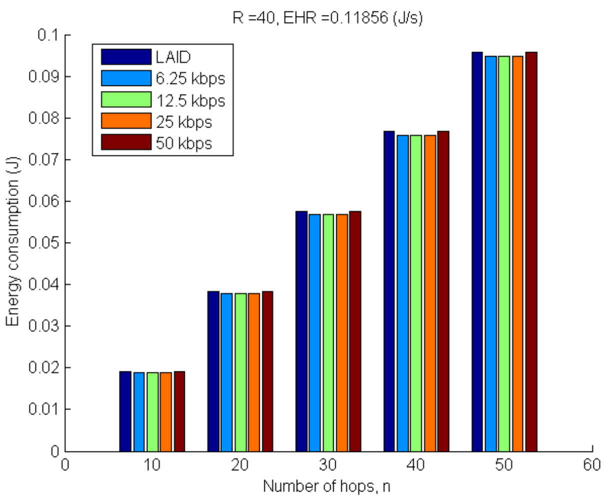

(b) Energy consumption vs the number of hops.

Fig. 7. Comparison of LAID, FDR6.25, FDR12.5, FDR25, and FDR50 when the number of hops varies.

so that loss of some encoded packets does not affect the recipient to recover the original IPv6 packet.

In addition to IEEE 802.15.4 standard based BF-WSNs, the proposed LAID may be applicable in other kinds of battery-free wireless networks. The key to the LAID is in solving the OP in (43) so as to find the optimal pairing of the data rate and the MNTT. Surely, it consumes energy to solve the OP. Hence, in practice, we should carefully consider when and where to solve the OP. The hint is to let the nodes solve the OP at a fixed interval, and the duration of the fixed interval depends on how much energy the nodes can harvest. In the extreme case when the energy consumed in solving the OP is considerably greater, compared to the harvested energy, we can let the gateway solve the OP and then piggyback the pairing of the optimal date rate and MNTT to the respective nodes.

REFERENCES

[1] S. Bandyopadhyay and A. Chandrakasan, "Platform architecture for solar, thermal, and vibration energy combining with mppt and single inductor," *IEEE Journal of Solid-State Circuits*, vol. 47, no. 9, pp. 2199-2215, Sep. 2012.

[2] Y. Yang, L. Su, Y. Gao, T.F. Abdelzaher, "SolarCode: Utilizing Erasure Codes for Reliable Data Delivery in Solar-powered Wireless Sensor Networks," *2010 Proceedings IEEE INFOCOM*, 2010, pp.1-5.

[3] M. Y. Naderi, P. Nintanavongsa, K. R. Chowdhury, "RF-MAC: A Medium Access Control Protocol for Re-Chargeable Sensor Networks Powered by Wireless Energy Harvesting," *IEEE Transactions on Wireless Communications*, vol. 13, no. 7, pp. 3926 C 3937, 2014.

[4] V. Liu, A. Parks, V. Talla, S. Gollakota, D. Wetherall, and J. R. Smith, "Ambient Backscatter: Wireless Communication Out of Thin Air," *SIGCOMM '13: Proceedings of the ACM SIGCOMM 2013 conference on SIGCOMM*, August 12-16, 2013, Hong Kong, China, pp. 39-50.

[5] P. C. Jain, "Recent Trends in Energy Harvesting for Green Wireless Sensor Networks," *International Conference on Signal Processing and Communication (ICSC)*, 2015, Noida, pp. 40-45.

[6] R. Gomez Cid-Fuentes, A. Cabellos-Aparicio, E. Alarcon, "Energy Buffer Dimensioning Through Energy-Erlangs in Spatio-Temporal-Correlated Energy-Harvesting-Enabled Wireless Sensor Networks," *IEEE Journal on Emerging and Selected Topics in Circuits and Systems*, vol. 4, no. 3, 2014, pp. 301-312.

[7] W. K. G. Seah, E. Z. Ang, and H. Tan, "Wireless sensor networks powered by ambient energy harvesting (WSN-HEAP) - Survey and challenges," *1st International Conference on Wireless Communication, Vehicular Technology, Information Theory and Aerospace & Electronic Systems Technology, 2009, Wireless VITAE 2009*, pp. 1-5.

[8] Y.-H. Zhu, S. Luan, V. C. M. Leung, and K. Chi, "Enhancing Timer-based Power Management to Support Delay-Intolerant Uplink Traffic in Infrastructure IEEE 802.11 WLANs," *IEEE Transactions on Vehicular Technology*, vol. 64, no. 1, pp. 386-399, 2015.

[9] H. Ma, L. Liu, A. Zhou, and D. Zhao, "On Networking of Internet of Things: Explorations and Challenges," *IEEE Internet of Things Journal*, DOI: 10.1109/JIOT.2015.2493082, 2015.

[10] N. Kushalnagar, G. Montenegro, and C. Schumacher, "IPv6 over Low-Power Wireless Personal Area Networks (6LoWPANs): Overview, Assumptions, Problem Statement, and Goals," RFC 4919, 2007.

[11] G. Montenegro, N. Kushalnagar, J. Hui, and D. Culler, "Transmission of IPv6 Packets over IEEE 802.15.4 Networks," RFC4944, 2007.

[12] Y.-H. Zhu, K. Chi, X. Tian, and V. C.M. Leung, "Network Coding Based Reliable IPv6 Packet Delivery over IEEE 802.15.4 Wireless Personal Area Networks," *IEEE Transactions on Vehicular Technology*, vol. 65, no. 4, pp. 2219-2230, 2016.

[13] X. Tian, Y. Zhu, and K. Chi, J. Liu, D. Zhang, "Reliable and Energy-efficient Data Forwarding in Industrial Wireless Sensor Networks," *IEEE Systems Journal*, DOI: 10.1109/JSYST.2015.2466696, 2015.

[14] J. Lei, R. Yates, and L. Greenstein, "A generic model for optimizing single-hop transmission policy of replenishable sensors," *IEEE Transactions on Wireless Communications*, vol. 8, no. 2, pp. 547-551, Feb. 2009.

[15] B. Medepally, N. B. Mehta, and C. R. Murthy, "Implications of energy profile and storage on energy harvesting sensor link performance," in*Proc. IEEE GLOBECOM*, Dec. 2009, pp. 1-6.

[16] C. K. Ho, P. D. Khoa, P. C. Ming, "Markovian models for harvested energy in wireless communications," *IEEE International Conference on Communication Systems (ICCS)*, 2010, pp. 311-315.

[17] E. Kavvadia, G. Koufoudakis, K. Oikonomou, "Robust Probabilistic Information Dissemination in Energy Harvesting Wireless Sensor Networks," *2014 13th Annual Mediterranean Ad Hoc Networking Workshop (MED-HOC-NET)*, 2014, pp. 63 C 70.

[18] J. Ventura and K. Chowdhury,"Markov modeling of energy harvesting Body Sensor Networks," *IEEE 22nd International Symposium on Personal Indoor and Mobile Radio Communications (PIMRC)*, 2011, pp. 2168-2172.

[19] J. A. Khan, H. K. Qureshi, A. Iqbal, "TRW: An Energy Storage Capacity Model for Energy Harvesting Sensors in Wireless Sensor Networks," *2014 IEEE 25th Annual International Symposium on Personal, Indoor, and Mobile Radio Communication (PIMRC)*, 2014, pp. 1931 -1936.

[20] A. Kansal, J. Hsu, S. Zahedi, M. B. Srivastava, "Power management in energy harvesting sensor networks," *ACM Transactions on Embedded Computing Systems*, vol. 6, pp. 32-es, 2007.

[21] J. R. Piorno, C. Bergonzini, D. Atienza, and T. S. Rosing, "Prediction and management in energy harvested wireless sensor nodes," *1st International Conference on Wireless Communication, Vehicular Technology, Information Theory and Aerospace & Electronic Systems Technology, 2009. Wireless VITAE 2009*, pp. 6-10.

[22] L. Longbi, N. B. Shroff, and R. Srikant, "Asymptotically Optimal Energy-Aware Routing for Multihop Wireless Networks With Renewable

This is the author's version of an article that has been published in this journal. Changes were made to this version by the publisher prior to publication.
The final version of record is available at http://dx.doi.org/10.1109/TMC.2016.2601906

Energy Sources," *IEEE/ACM Transactions on Networking*, vol. 15, pp. 1021-1034, 2007.

[23] M. Tacca, P. Monti, and A. Fumagalli, "Cooperative and reliable ARQ protocols for energy harvesting wireless sensor nodes," *IEEE Transactions on Wireless Communications*, vol. 6, no. 7, pp. 2519-2529, Jul. 2007.

[24] M. Mutschlechner, Bijun Li, R. Kapitza, F. Dressler, "Using Erasure Codes to overcome reliability issues in energy-constrained sensor networks." *2014 11th Annual Conference on Wireless On-demand Network Systems and Services (WONS)*, 2014, pp. 41-48.

[25] M. S. Srouji, Zhonglei Wang, and J. Henkel, "RDTS: A Reliable Erasure-Coding Based Data Transfer Scheme for Wireless Sensor Networks," *IEEE 17th International Conference on Parallel and Distributed Systems (ICPADS)*, 2011, pp. 481-488.

[26] I. Salhi, Y. Ghamri-Doudane, S. Lohier, G. Roussel, "Reliable Network Coding for ZigBee Wireless Sensor Networks," *2011 IEEE 8th International Conference on Mobile Adhoc and Sensor Systems (MASS)*, 2011, pp. 135-137.

[27] X. Wang, Y. Tan, Z. Zhou, L. Zhou, "Reliable and Energy-Efficient Multicast Based on Network Coding for Wireless Sensor Networks," *2011 6th International ICST Conference on Communications and Networking in China (CHINACOM)*, 2011, pp. 1142-1145.

[28] A. Apavatjrut, K. Jaffres-Runser, C. Goursaud, J.-M. Gorce, "Combining LT codes and XOR network coding for reliable and energy efficient transmissions in wireless sensor networks," *2012 35th IEEE Sarnoff Symposium (SARNOFF)*, 2012, pp.1-6.

[29] Y.-H. Zhu, J. Xu, E. Li, L. Xu, "Energy-efficient Reliable Data Gathering Scheme Based on Enhanced Reed-Solomon Code for Wireless Sensor Networks," *2014 International Conference on Smart Computing (SMARTCOMP)*, 2014, pp. 275-280.

[30] B. Luo, Z. Sun, "Enabling End-to-End Communication Between Wireless Sensor Networks and the Internet Based on 6LoWPAN," *Chinese Journal of Electronics*, vol.24, no.3, pp. 633-638, 2015.

[31] A. Ludovici, A. Calveras, J. Casademont, "Forwarding Techniques for IP Fragmented Packets in a Real 6LoWPAN Network," *Sensors*, vol.11, no.1, pp. 992-1008, 2011.

[32] J.W. Hui, D.E. Culler, "IPv6 in Low-Power Wireless Networks," *Proceedings of the IEEE*, vol.98, no.11, pp. 1865-1878, 2010.

[33] N. Sagar, S. Shyam Sunder, P. C. Reddy, C. Sumana, "Analysis on Range Enhancing Energy Harvester (Reach) Mote Passive Wake-Up Radios for Wireless Networks," *49th Annual Convention of Computer-Society-of-India - Emerging ICT for Bridging the Future*, 2015.

[34] Z. A. Eu, H.-P. Tan, and W. K.G. Seah, "Opportunistic routing in wireless sensor networks powered by ambient energy harvesting," *Computer Networks*, vol. 54, pp. 2943 C 2966, 2010.

[35] Y. Li and J. Shao, "Optimized Resource Allocation for Utility-Based Routing in Ad Hoc and Sensor Network," *KSII Transactions on Internet and Information Systems*, vol. 9, no.5, pp. 1790-1806, 2015.

[36] IEEE Computer Society, "IEEE 802.15.4 Standard for Wireless Medium Access Control (MAC) and Physical Layer (PHY) Specifications for Low-Rate Wireless Personal Area Networks (WPANs)", 2011.

[37] A. P. Sample, D. J. Yeager, P. S. Powledge, A. V. Mamishev, J. R. Smith, "Design of an RFID-based battery-free programmable sensing platform," *IEEE Transactions on Instrumentation and Measurement*, 2008, vol. 57, no. 11, pp. 2608-2615.

[38] W. B. Heinzelman, A. P. Chandrakasan, and H. Balakrishnan, "An application-specific protocol architecture for wireless microsensor networks," *IEEE Transactions on Wireless Communications*, vol. 1, pp. 660-670, 2002.

[39] N. F. Timmons and W. G. Scanlon, "Analysis of the performance of IEEE 802.15.4 for medical sensor body area networking," *First Annual IEEE Communications Society Conference on Sensor and Ad Hoc Communications and Networks*, 2004. IEEE SECON 2004, pp. 16-24.

[40] LAN/MAN Standards Committee, "Part 15.4: Low-Rate Wireless Personal Area Networks (LR-WPANs) Amendment 3: Physical Layer (PHY) Specifications for Low Data-Rate, Wireless, Smart Metering Utility Networks," 2012.

[41] Y.-H. Zhu, H. Lu, and V. C.M. Leung, "Access Point Buffer Management for Power Saving in IEEE 802.11 WLANs," *IEEE Transactions on Network and Service Management*vol. 9, no. 4, pp. 473-486, Dec. 2012.

[42] G. Martinez, S. Li, C. Zhou, "Wastage-Aware Routing in Energy-Harvesting Wireless Sensor Networks", *IEEE Sensors Journal*, vol. 14, pp.2967-2974, 2014.

[43] U.S. Dept. of Energy, "National Solar Radiation Database", http://rredc.nrel.gov/solar/old_data/nsrdb/.

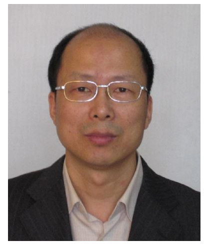

Yi-hua Zhu (M01-SM07) received his B.S. degree in mathematics from Zhejiang Normal University, Zhejiang, China, in July 1982; his M.S. degree in operation research and cybernetics from Shanghai University, Shanghai, China in April 1993; and his Ph.D. degree in computer science and technology from Zhejiang University, Zhejiang, China, in March 2003. Dr. Zhu is a professor at Zhejiang University of Technology, Hangzhou, Zhejiang, China. He is a member of China Computer Federation Technical Committee on Sensor Network. His current research interests include information dissemination, stochastic modeling and analysis, power management, mobility management for wireless networks, and network coding. He has served as technical program committee members or co-chairs in the international conferences IEEE ICC, WCNC, GlobeCom, DCOSS, etc. He is the recipient of the Best Paper Award of Chinacom 2008. He has published more than 170 research papers in proceedings and journals including IEEE Transactions on Wireless Communications, IEEE Transactions on Vehicular Technology, and more.

Shu-Wei Qiu received his B.S. degree from Hanshan Normal University, Chaozhou, China, in 2003; his M.S. degree from Guangdong University of Technology, Guangzhou, China, in 2009. He is currently a candidate student for his Ph.D degree in Zhejiang University of Technology. His current research interests include information dissemination for wireless networks, especially for battery-free wireless sensor networks and wireless local area networks.

Kaikai Chi received the B.S. and M.S. degrees from Xidian University, Xi'an, China, in 2002 and 2005, respectively, and the Ph.D. degree from Tohoku University, Sendai, Japan, in 2009. He is currently an associate professor in the School of Computer Science and Technology, Zhejiang University of Technology, Hangzhou, China. His current research focuses on wireless ad hoc network and wireless sensor network. He was the recipient of the Best Paper Award at the IEEE Wireless Communications and Networking Conference in 2008. He has published more than 30 referred technical papers in proceedings and journals like IEEE Transactions on Wireless Communications and IEEE Transactions on Parallel and Distributed Systems.

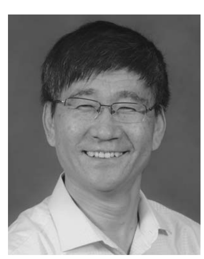

Yuguang "Michael" Fang (F'08) received the M.S. degree from Qufu Normal University, China, in 1987, and Ph.D. degrees from both Case Western Reserve University, Cleveland, OH, USA and Boston University, Boston, MA, USA, in 1994 and 1997,respectively. He joined the Department of Electrical and Computer Engineering, University of Florida,FL, USA, in 2000 and has been a Full Professor since 2005. He received the US NSF CAREER Award in 2001, the US ONR Young Investigator Award in 2002, 2015 IEEE Communications Society CISTC Technical Recognition Award, 2014 IEEE Communications Society WTC Recognition Award, and is a recipient of the Best Paper Award in IEEE International Conference on Network Protocols in 2006. He also received a 2010C2011 UF Doctoral Dissertation Advisor/Mentoring Award. He served as the Editor-in-Chief of IEEE Wireless Communications and is currently serving as the Editor-in-Chief of IEEE TRANSACTIONS ON VEHICULAR TECHNOLOGY. He is a Fellow of IEEE.